

Targeting Long Noncoding RNA HMMR-AS1 Suppresses and Radiosensitizes Glioblastoma



Junyang Li¹, Xiangjun Ji¹ and Handong Wang

Department of Neurosurgery, Jinling Hospital, Medical School of Nanjing University, Nanjing, 210002, China

Abstract

Emergent evidences revealed that long noncoding RNAs (lncRNAs) participate in neoplastic progression. *HMMR* is an oncogene that is highly expressed in glioblastoma (GBM) and supports GBM growth. Whether lncRNAs regulate *HMMR* in GBM remains unknown. Herein, we identify that an *HMMR* antisense lncRNA, HMMR-AS1, is hyperexpressed in GBM cell lines and stabilizes *HMMR* mRNA. Knockdown of HMMR-AS1 reduces HMMR expression; inhibits cell migration, invasion, and mesenchymal phenotypes; and suppresses GBM cell growth both *in vitro* and *in vivo*. Moreover, knockdown of HMMR-AS1 radiosensitizes GBM by reducing DNA repair proteins ATM, RAD51, and BMI1. Our data demonstrate a mechanism of sense-antisense interference between *HMMR* and HMMR-AS1 in GBM and suggest that targeting HMMR-AS1 is a potential strategy for GBM treatment.

Neoplasia (2018) 20, 456–466

Introduction

Glioblastoma (GBM) is the most malignant brain tumor in adults, with a median survival of less than 2 years [1]. Despite the current aggressive treatments including accurate surgical section with multiple assistive techniques, normalized radiotherapy, and adjuvant TMZ chemotherapy, recurrence is inevitable and the prognosis remains poor [2]. Although clinical studies are needed to establish optimal therapeutic strategies for GBM, studies at the cellular and molecular levels are equally needed to find better therapeutic targets [3].

Hyaluronan-mediated motility receptor (*HMMR*) is well known as a breast cancer susceptibility oncogene that plays key roles during the neoplastic progression. Hyperexpression of HMMR has been reported in multiple cancers, including GBM, which is associated with poor outcome of patients [4–8]. Tilghman et al. found that HMMR supports the self-renewal and tumorigenic potential of GBM stem cells, suggesting HMMR as a novel therapeutic target for inhibiting glioblastoma [4]. Besides direct targeting *HMMR* by small interfering RNA (siRNA), finding other genes that regulate *HMMR* may also benefit GBM treatment.

Recently, more and more evidences declared that noncoding RNAs (ncRNAs) play key roles in human cancer biology [9]. Those ncRNA molecules longer than 200 nucleotides are named as long noncoding RNAs (lncRNAs), regulating mRNA translation, transcriptional processes and cell development, proliferation, and apoptosis [10–12]. Antisense transcription is from the opposite strand of a protein-coding gene or a sense strand-derived RNA. Some have demonstrated that more than 63% of transcripts have antisense partners, most of which are noncoding RNAs [13,14]. Antisense

lncRNAs can function as positive and negative modulators of coding genes [15]. Several antisense lncRNAs, such as HOTAIR, TSLC1-AS1, and HIF1A-AS2, have been demonstrated to affect glioma growth [16–20]. The nature antisense partner of *HMMR* is a noncoding RNA named as *HMMR* antisense RNA 1 (HMMR-AS1). As far as we know, whether HMMR-AS1 regulates *HMMR* in GBM and the underlying molecular mechanisms remain unclear.

In the present study, we investigated the effects of HMMR-AS1 on GBM *in vitro* and *in vivo*. We found that HMMR-AS1 is elevated in GBM cell lines and stabilizes *HMMR* mRNA. Knockdown of HMMR-AS1 decreases HMMR mRNA and protein levels; suppresses cell proliferation, migration, and invasion; and reduces expression of ataxia telangiectasia mutated kinase (ATM), RAD51, and BMI1 which are required for efficient homologous repair (HR) of DNA double-strand breaks (DSBs). We built a GBM intracranial xenograft model and found that knockdown of HMMR-AS1 inhibits

Abbreviations: GBM, glioblastoma; HMMR, hyaluronan-mediated motility receptor; lncRNA, long noncoding RNA; HMMR-AS1, HMMR antisense RNA 1; DSBs, double-strand breaks; ATM, ataxia telangiectasia mutated kinase; HR, homologous repair. Address all correspondence to: Handong Wang, 305 East Zhongshan Road, Nanjing, 210002, China. E-mail: njhdwang@hotmail.com

¹ These authors contributed equally to this work.

Received 11 January 2018; Revised 11 February 2018; Accepted 14 February 2018

© 2018 The Authors. Published by Elsevier Inc. on behalf of Neoplasia Press, Inc. This is an open access article under the CC BY-NC-ND license (<http://creativecommons.org/licenses/by-nc-nd/4.0/>).

1476-5586/18

<https://doi.org/10.1016/j.neo.2018.02.010>

GBM growth and radiosensitizes GBM *in vivo*. Our data identified this long noncoding RNA HMMR-AS1 regulating *HMMR* and inhibiting GBM propagation.

Materials and Methods

Reagents and Antibodies

The inhibitor of RNA polymerase II/III, α -amanitin, was purchased from MedChem Express (Monmouth Junction, NJ). The luciferin (*in vivo* grade) used for animal experiments was purchased from Promega (Madison, WI). For Western blot analysis, the primary antibodies against β -actin, c-Myc, BMI1, p27 Kip1, Cyclin D1, CDK2, CDK4, ERK1/2, p-ERK1/2(Thr202/Tyr204), ZEB1, β -Catenin, N-Cadherin, Vimentin, ATM, p-ATM, and Rad51 were all purchased from Cell Signaling Technology (Beverly, MA); HMMR#1 was purchased from OriGene (Rockville, MD); and HMMR#2 was purchased from GeneTex (Irvine, CA). For immunohistochemical (IHC) staining, the primary antibody HMMR#1 was purchased from Origene (Rockville, MD), ZEB1 was from Abcam (Cambridge, MA), and β -Catenin and Vimentin were purchased from Cell Signaling Technology (Beverly, MA).

Cell Culture

Human glioblastoma cell lines U87, U251, A172, and U118 were purchased from CBTC CAS (Cell Bank, Type Culture Collection of Chinese Academy of Sciences). Human astrocyte cell line HA was provided by China Infrastructure of Cell Line Resources (Beijing Headquarters). All glioblastoma cell lines were cultured in Dulbecco's modified Eagle's medium supplemented with 10% fetal bovine serum and 1% penicillin-streptomycin. HA cells were cultured in complete astrocyte medium containing 1% astrocyte growth supplement, 2% fetal bovine serum, and 1% penicillin-streptomycin (ScienCell, Carlsbad, CA). Cells were maintained at 37°C in a humidified atmosphere of 95% air and 5% CO₂.

siRNA Transfection

Cells were transiently transfected with siRNAs against human HMMR-AS1 or *HMMR* using Lipofectamine 3000 transfection reagent (Life Technologies) according to the manufacturer's instructions. HMMR-AS1 and *HMMR* siRNA duplexes were designed and generated by HanBio Co., Ltd. (Shanghai, China). The siRNA sequences mentioned above were as follows: siRNA-*HMMR* (sense: CCCUAAUGCUCACCUUUAUTT, antisense: AUAAAGGUGAGCAUUAGGGTT); siRNA-HMMR-AS1 (sense: UGGAGAAGCU-GAAGCCUAATT, antisense: UUAGGCUUCAGCUUCUCCATT); negative control (sense: UUCUCCGAACGUGUCACGUTT, antisense: ACGUGA CACGUUCGGAGAATT).

Lentiviral Infection for Short Hairpin RNA (shRNA) and Gene Transfection

To establish stable *HMMR* or HMMR-AS1 knockdown cells, lentivirus-based shRNA targeting human *HMMR* or HMMR-AS1 was generated and transfected into cells. Lentivirus containing *HMMR* or HMMR-AS1 full-length sequences was transfected into cells for stable overexpression of *HMMR* or HMMR-AS1. Lentivirus containing luciferase sequence was transfected into U87 cells (U87-luc cells) for *in vivo* study. All lentiviral vectors mentioned above were generated by HanBio Co., Ltd. (Shanghai, China). The shRNA sequences mentioned above were as follows: shRNA-*HMMR*,

GAGTCTTCATCAGAAGCTCTGTTCT; shRNA-HMMR-AS1, GAAGAGATTAGTGCCACCATAAGTA.

Cell Survival and Proliferation Assay

Cell Counting Kit-8 (CCK-8 kit) purchased from Dojindo Laboratories (Kumamoto, Japan) was used for cell survival and proliferation assay. For cell survival assay, cells were transplanted into 96-well plates followed by different treatments; then culture medium was discarded, and cells were cultured in 100 μ l fresh serum-free medium that contained 10 μ l CCK-8 solutions for 2 hours. Then, the 96-well plate was put into an enzyme-linked immunosorbent assay plate reader (Bio-Rad Laboratories, Inc., Berkeley, CA), and optical density values (absorbance) were recorded at 450 nm. The relative cell survival rate was calculated according to the absorbance compared with control. For cell proliferation assay, differently transfected cells were transplanted into 96-well plates and allowed cell growth for 4 days. Optical density values were recorded each day, and the relative cell proliferation was calculated based on the ratios of absorbance to the baseline absorbance at day 1.

Cell Migration and Invasion Assays

For cell migration assay, cells were transplanted into 24-well Transwell chambers (8- μ m pore size, Corning) without Matrigel in serum-free Dulbecco's modified Eagle's medium. Conditioned medium was cultured into the lower chambers like chemoattractants, while cells in the upper chambers were differently treated. After 18-hour incubation, cells on upper surface of filters were scraped by a cotton swab, whereas cells adherent to the bottom of membrane were fixed by methanol and stained by 0.1% crystal violet. For cell invasion assay, the procedure is the same as migration assay except for coating the upper surface of filters by Matrigel (Corning) before use. Stained cells were observed and pictures were taken using a Zeiss Axio Scope. A1 microscope (Carl Zeiss, Oberkochen, Germany).

Cell Cycle Analysis by Flow Cytometry

Cell cycle analysis was performed using a FACS Calibur flow cytometer (BD Biosciences, San Jose, CA) as we described previously [21]. Briefly, cells transfected with siRNA targeting HMMR-AS1 were harvested and fixed by 75% ethanol. Cell nuclei were analyzed after staining using propidium iodide.

Cellular Immunofluorescence Assay

Cellular immunofluorescence assay was performed as we described previously [21]. Briefly, differently transfected cells were attached on coverslips, fixed by 4% paraformaldehyde, and probed with primary antibody HMMR#1 (OriGene, Rockville, MD) at 4°C overnight followed by incubation with Cy5-labeled secondary antibody (Jackson ImmunoResearch Laboratories, Inc., West Grove, PA) for 60 minutes at room temperature. DAPI (Beyotime Biotechnology, Shanghai, China) was used for staining nuclei.

Quantitative Real-Time PCR Assay

Total RNA was extracted from samples by using Trizol (Invitrogen), and then the RNA was reverse transcribed to form cDNA by SuperScript III Reverse Transcriptase (Invitrogen) as we described previously [21]. The qRT-PCR assay was performed in an ABI 7300 real-time PCR system (Applied Biosystems). The primers were: *HMMR* (forward: CATGGTGCAGCTCAGGAACA; reverse: AAGCTGA CAGCGGAGTTTTG); HMMR-AS1 (forward: AACTCGCCTATT

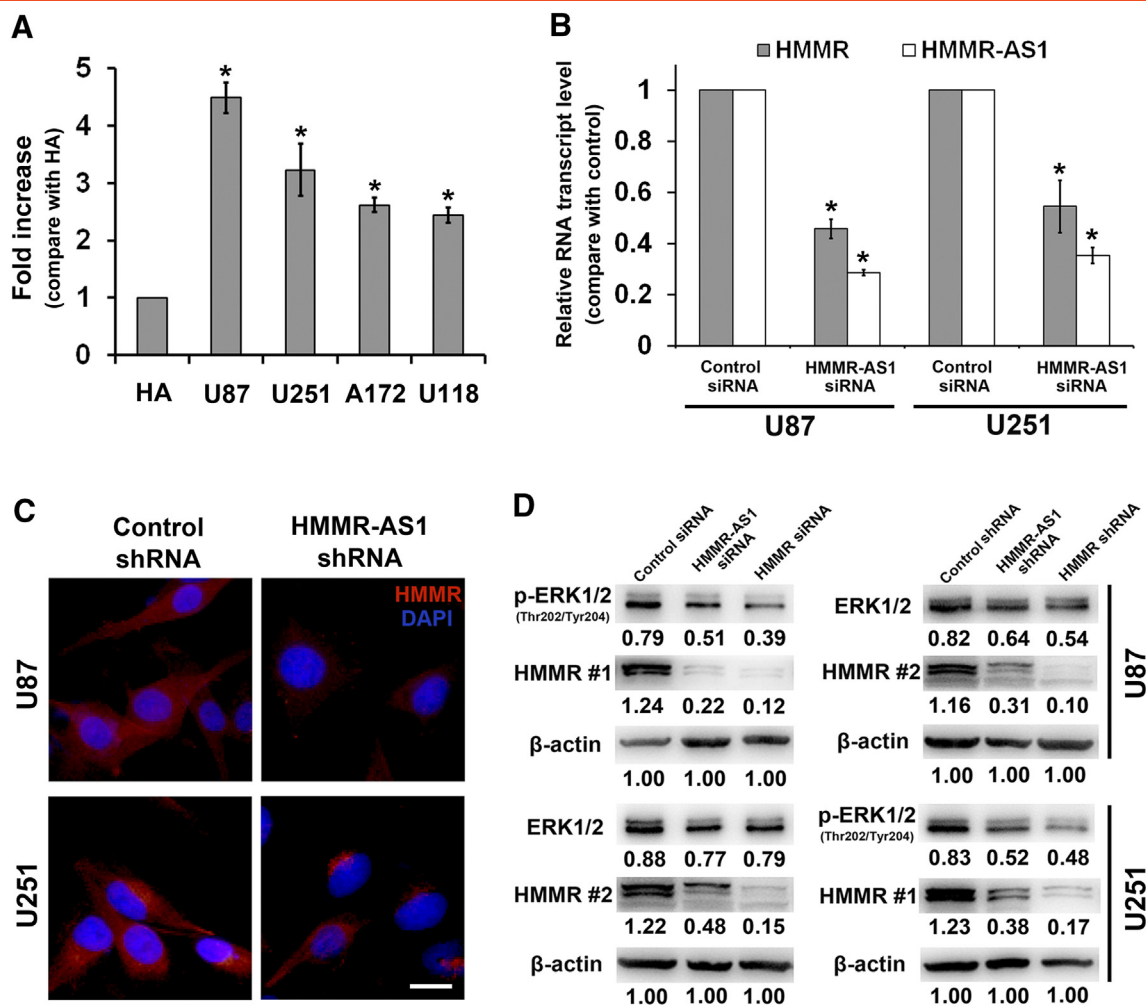


Figure 1. HMMR-AS1 is elevated in GBM cell lines and regulates HMMR expression. (A) Relative levels of HMMR-AS1 transcript in GBM cell lines U87, U251, A172, and U118 compared with normal human astrocyte cell line HA, which were represented as fold increases. (B) Relative levels of HMMR mRNA or HMMR-AS1 transcript in U87 and U251 cells treated with siRNA targeting HMMR-AS1. (C) HMMR expression analyzed by immunofluorescence in U87 and U251 cells transfected with HMMR-AS1 shRNA. Scale bar = 10 μ m. (D) Knockdown of HMMR-AS1 by siRNA or shRNA reduces expression of HMMR and ERK1/2 and phosphorylation of ERK1/2. Knockdown of *HMMR* was used as positive control. Two HMMR antibodies purchased from different companies were used (HMMR#1 and #2). * $P < .05$. β -Actin was used as a loading control for Western blot. The blot bands were quantified by ImageJ and represented by relative values compare with loading control (1.00).

TAGCCTGGG; reverse: ATACCAGGAACCAGGAGTTGTGT); β -actin (forward: CACCCAGCACAATGAAGATCAAGAT; reverse: CCAGTTTTTAAATCCTGAGTCAAGC). Data analysis was performed using $\Delta\Delta C_t$ (threshold cycle normalized by β -actin compare with control) method, and the fold-change was calculated as $2^{-\Delta\Delta C_t}$.

RNA Stability Assay

U87 cells stably expressing control shRNA, HMMR-AS1 shRNA, or *HMMR* shRNA were planted into six-well plates. To test the RNA stability, we treated cells with 50 μ M α -amanitin and harvested cells for qRT-PCR at 6, 12, and 18 hours posttreatment.

Western Blot Analysis

Western blot analysis was performed as we described previously [21]. Briefly, the whole cell lysates were separated by SDS-PAGE and transferred to a polyvinylidene difluoride membrane. Membranes were then incubated with primary antibodies followed by secondary antibody. Immunoblots of proteins were visualized with chemilumi-

nescent detection kit (Millipore, MA, USA). Public software ImageJ (National Institutes of Health, USA) was used to quantify the densitometry of the immunoblotting bands.

Glioblastoma Intracranial Xenograft Model

This study was approved by the institutional animal care and use committee of Jinling Hospital. First of all, U87 cells expressing luciferase (U87-luc cells) were transfected with HMMR-AS1 shRNA or control shRNA before implantation. Then, approximately 5.0×10^5 U87-luc (control shRNA or HMMR-AS1 shRNA) cells were transplanted into the right striatum of BALB/c nude mice (male at 5 to 6 weeks old) to develop a intracranial xenograft model of human glioblastoma. Tumor growth was monitored by bioluminescence using an *in vivo* living imaging system (IVIS Spectrum, PerkinElmer, Waltham, MA). Mice were sacrificed, and the brain tissues containing tumors were extracted, fixed, and embedded in paraffin for IHC staining.

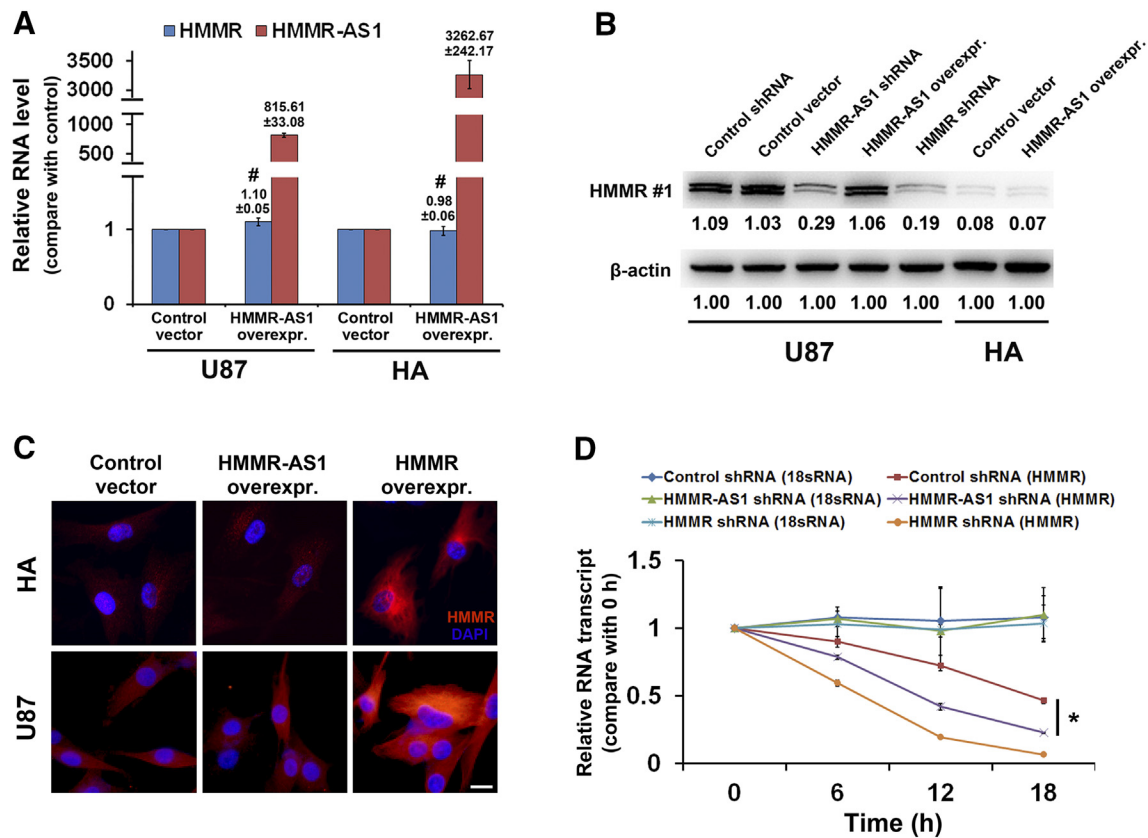


Figure 2. HMMR-AS1 stabilizes *HMMR* mRNA. (A) Relative levels of HMMR-AS1 and HMMR mRNA in U87 and HA cells transfected with lentivirus containing HMMR-AS1 full-length sequence compare with control. (B) HMMR protein expression tested by Western blot in cells that HMMR-AS1 was downregulated or upregulated. (C) HMMR protein expression tested by immunofluorescence in control cells or cells with HMMR-AS1 or *HMMR* overexpression. Scale bar = 10 μ m. (D) U87 cells differently transfected were treated with 50 μ M α -amanitin for 6, 12, or 18 hours. Cells were then harvested for qRT-PCR to test the loss of *HMMR* mRNA. 18s RNA, a product of RNA polymerase I, was not affected by α -amanitin. Cells transfected with *HMMR* shRNA were used as positive control. β -Actin was used as a loading control for Western blot. The blot bands were quantified by ImageJ and represented by relative values compare with loading control (1.00). # $P > .05$, * $P < .05$. HA: human astrocyte cell line; overexpr.: overexpression.

X-Ray Irradiation

Irradiation was performed at room temperature in an RS-2000 Pro Biological Irradiator (Radsources, Buford, GA) at a dose rate of 2.13 Gy/min (maximum energy of 160 kV and 25 mA).

IHC Staining

The whole brain tissues containing tumors were obtained and paraffin-embedded. The specimen was cut as 4- μ m-thick sections, and the paraffin-embedded tissue sections were deparaffinized, treated with 3% H_2O_2 , and incubated with the primary antibody followed by incubation with HRP-labeled secondary antibody. The visualization signal was developed with 3,3'-diaminobenzidine, and then tissue sections were observed and pictures were taken.

Statistical Analysis

The SPSS, GraphPad Prism, and Microsoft Excel were used for statistical analysis. Comparisons between two groups were carried out using one-way analysis of variance or independent t test, and expressed as mean \pm standard error. $P < .05$ was considered statistically significant.

Results

HMMR-AS1 Regulates HMMR Expression

We analyzed the levels of HMMR-AS1 transcript in human glioblastoma cell lines, U87, U251, A172, and U118, and a normal human astrocyte cell line, HA, and found that HMMR-AS1 is elevated in glioblastoma cells compared with HA (Figure 1A). Then, to investigate the effects of HMMR-AS1 on GBM cells, siRNA sequences targeting HMMR-AS1 were transiently transfected into U87 and U251 cells to knock down HMMR-AS1 expression. In transfected cells, we found not only the knockdown of targeted HMMR-AS1 transcript but also the downregulation of *HMMR* mRNA (Figure 1B) and protein levels (Figure 1D). The results in U87 and U251 cell lines expressing HMMR-AS1 shRNA also showed that HMMR protein is significantly reduced by knockdown of HMMR-AS1 (Figure 1, C and D). Two antibodies against HMMR (HMMR #1 and #2) produced by two different companies were used to make the data credible. The results of cellular immunofluorescence confirmed that HMMR expression was reduced in cells transfected with HMMR-AS1 shRNA (Figure 1C). The levels of ERK1/2 and phosphorylated ERK1/2, which have been demonstrated to be regulated by HMMR [4], were also reduced by knockdown of HMMR-AS1 (Figure 1D).

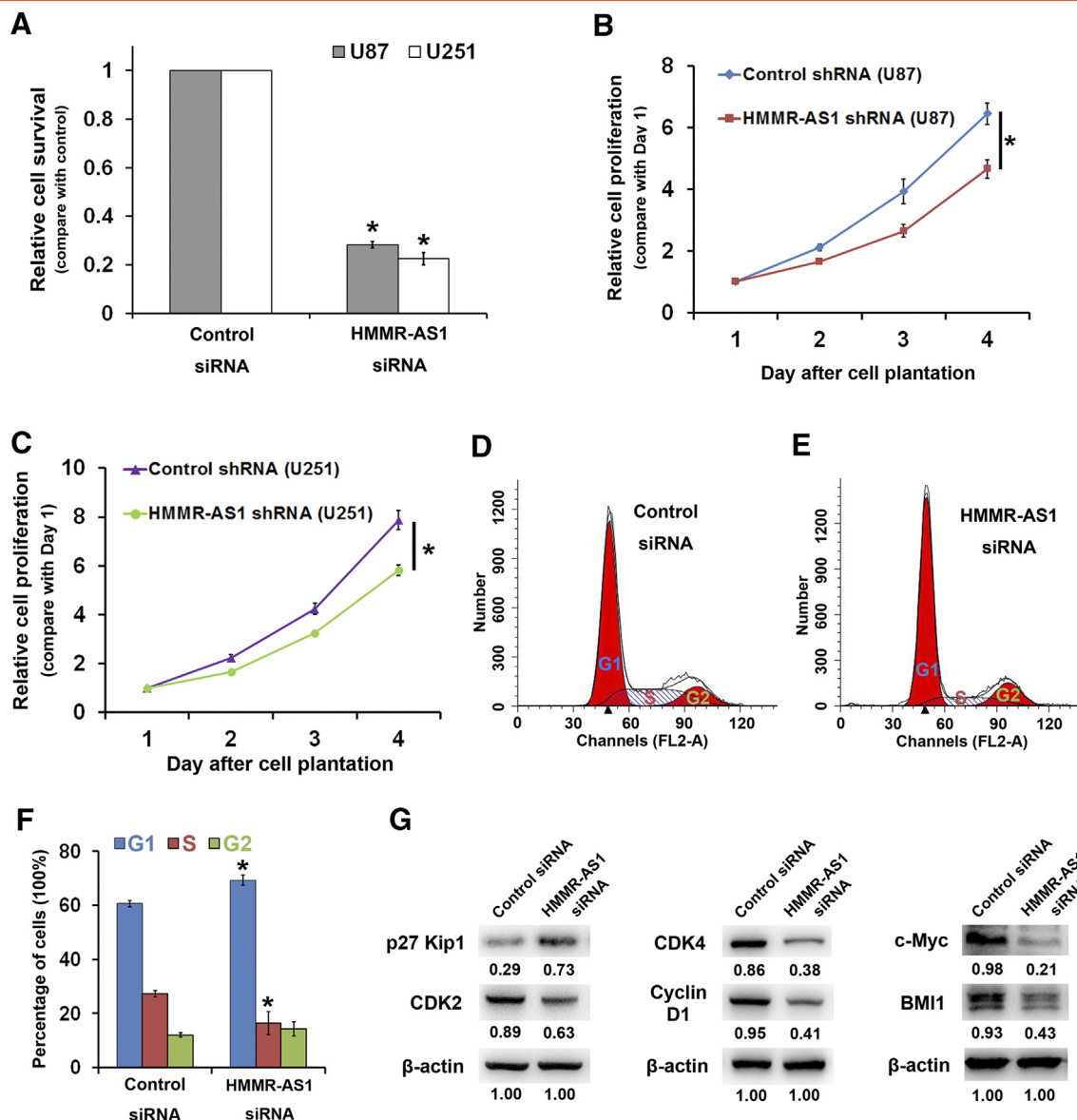


Figure 3. Knockdown of HMMR-AS1 inhibits cell growth and induces cell cycle G1 phase arrest. (A) Cells were transfected with control siRNA or siRNA targeting HMMR-AS1, and cell survival was detected by using CCK-8 kit. U87 (B) or U251 (C) cells were transfected with HMMR-AS1 shRNA and planted in 96-well plates for 4 days. Cell proliferation was detected by using CCK-8 kit every day. U87 cells were transfected with control siRNA (D) or siRNA targeting HMMR-AS1 (E), and cell cycle was analyzed by flow cytometry (F). (G) Several cell cycle regulators were detected by Western blot analysis. β -Actin was used as a loading control. The blot bands were quantified by ImageJ and represented by relative values compared with loading control (1.00). * $P < .05$.

HMMR-AS1 Stabilizes HMMR mRNA

In U87 or HA cell line stably transfected with full-length sequence of HMMR-AS1, overexpression of HMMR-AS1 did not increase HMMR mRNA (Figure 2A) or protein level (Figure 2, B and C). We assume that, as a nature antisense transcript, HMMR-AS1 may act to stabilize the HMMR transcript rather than elevate it. To assess the effects of HMMR-AS1 on HMMR stability, we used an inhibitor of RNA polymerase II/III, α -amanitin, to block new RNA synthesis and measured the loss of HMMR after 18 hours. The loss of HMMR mRNA in U87 cells expressing HMMR-AS1 shRNA is faster than that in control cells, indicating that depletion of HMMR-AS1 decreases the stability of HMMR transcript (Figure 2D).

HMMR-AS1 Affects GBM Cell Proliferation, Migration, and Invasion

To investigate the effects of HMMR-AS1 on GBM cell growth, we treated U87 and U251 cells with HMMR-AS1 siRNA for 72 hours. The results showed that siRNA targeting HMMR-AS1 significantly inhibits cell survival (Figure 3A). Then, we investigated whether stable transfection of HMMR-AS1 shRNA affects the proliferation of U87 and U251 cells. Cells were allowed to grow for 4 days. We found that the proliferation of cells transfected with HMMR-AS1 shRNA is significantly inhibited (Figure 3, B and C).

Next, we analyzed the cell cycle of U87 cells transfected with HMMR-AS1 siRNA by using flow cytometry. We found that siRNA targeting HMMR-AS1 increases cells in G1 phase and decreases cells in S phase (Figure 3, D-F). We measured the levels of several cell cycle

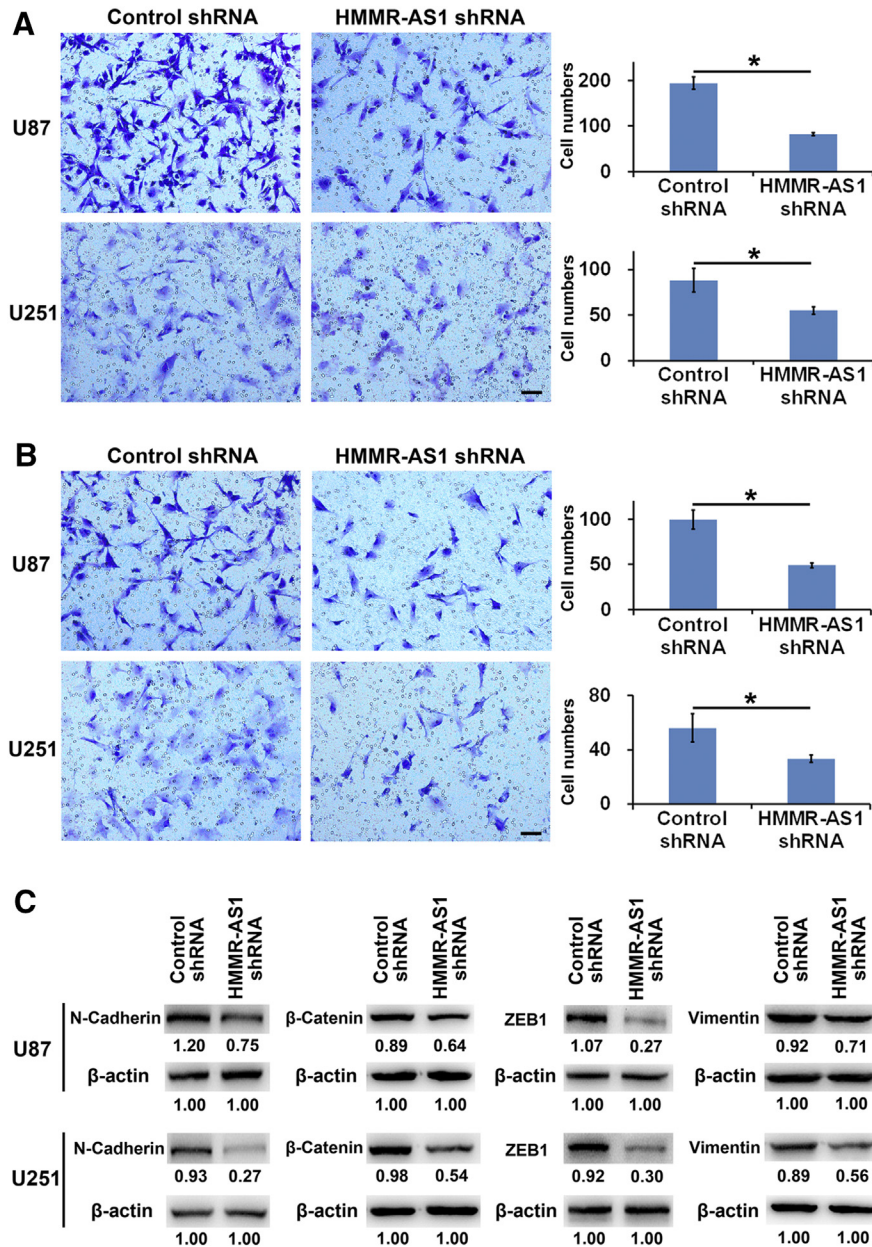


Figure 4. Knockdown of HMMR-AS1 inhibits cell migration and invasion. U87 and U251 cells were transfected with control shRNA or HMMR-AS1 shRNA. (A) Cell migration was analyzed by using Transwell chambers without Matrigel. Scale bar = 50 μ m. (B) Cell invasion was analyzed by using Matrigel-coated Transwell chambers. Scale bar = 50 μ m. (C) Expression of mesenchymal phenotypes in cells transfected with HMMR-AS1 shRNA was detected by using Western blot. β -Actin was used as a loading control. The blot bands were quantified by ImageJ and represented by relative values compare with loading control (1.00). * $P < .05$.

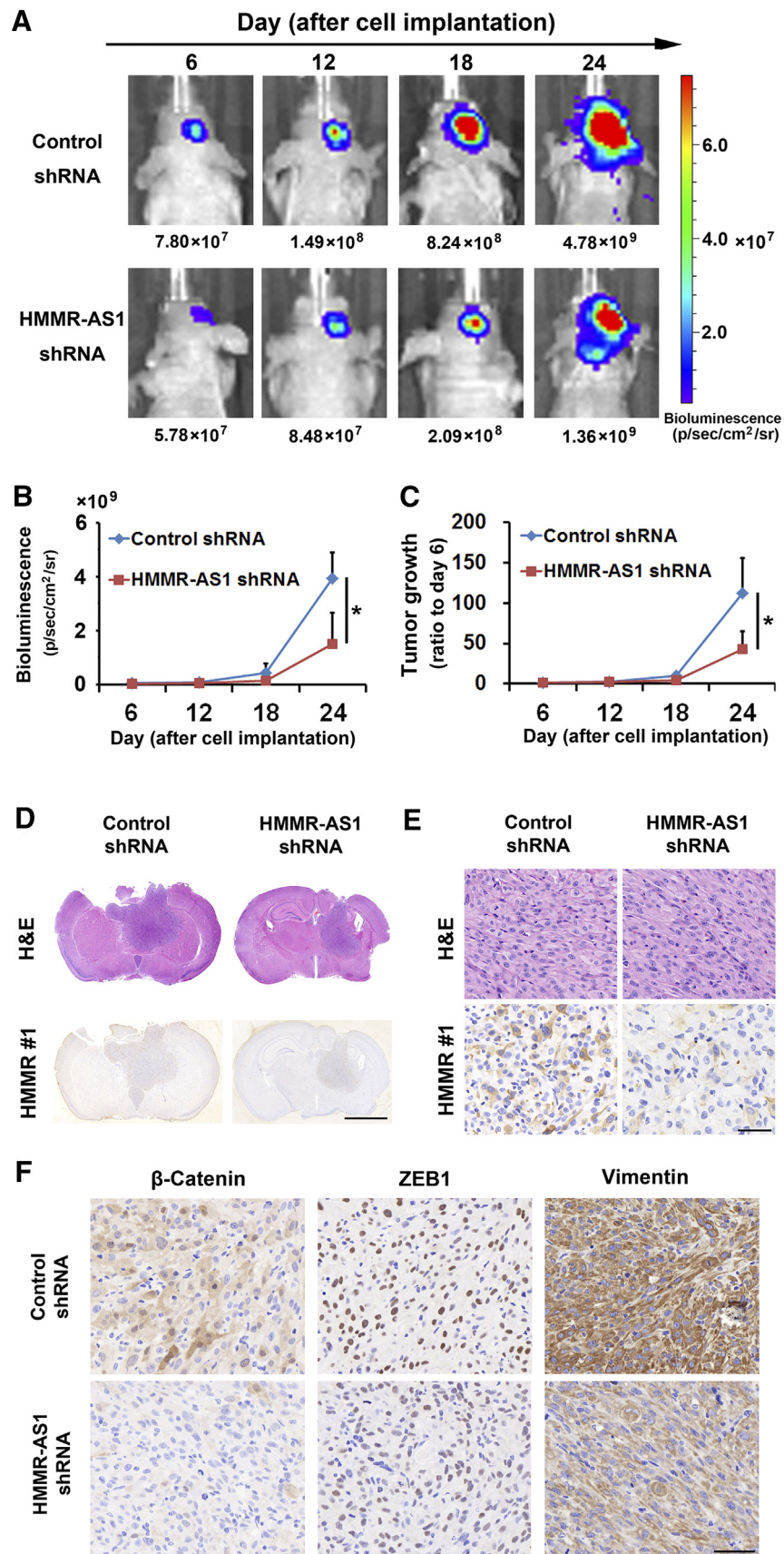
regulators and found that siRNA transfection increases p27 Kip1 level and decreases expression of CDK2, c-Myc, BMI1, Cyclin D1, and CDK4 (Figure 3G). These results indicated that knockdown of HMMR-AS can block cells to pass the restriction (R) point which is necessary for G1 phase progression and S phase entry and arrest cells in cell cycle G1 phase.

Then, we assessed cell migration and invasion by using Transwell chambers. Cells expressing HMMR-AS1 shRNA were transplanted into the chambers for analysis. Our data showed that knockdown of HMMR-AS1 impairs both cell migratory (Figure 4A) and invasive capability (Figure 4B). We also found that knockdown of

HMMR-AS1 reduces expression of mesenchymal phenotypes, such as N-cadherin, β -Catenin, ZEB1, and Vimentin (Figure 4C).

HMMR-AS1 Affects GBM Growth In Vivo

To investigate whether knockdown of HMMR-AS1 inhibits glioblastoma growth *in vivo*, we built a glioblastoma intracranial xenograft model. U87-luc cells transfected with control shRNA or HMMR-AS1 shRNA were separately transplanted into the right striatum of nude mice, and tumor growth was monitored by bioluminescence *in vivo* imaging. The bioluminescence signal was captured at day 6, 12, 18, and 24 after cell implantation, and the signal intensity represented the size of transplanted tumor. Our data showed that tumors are smaller in



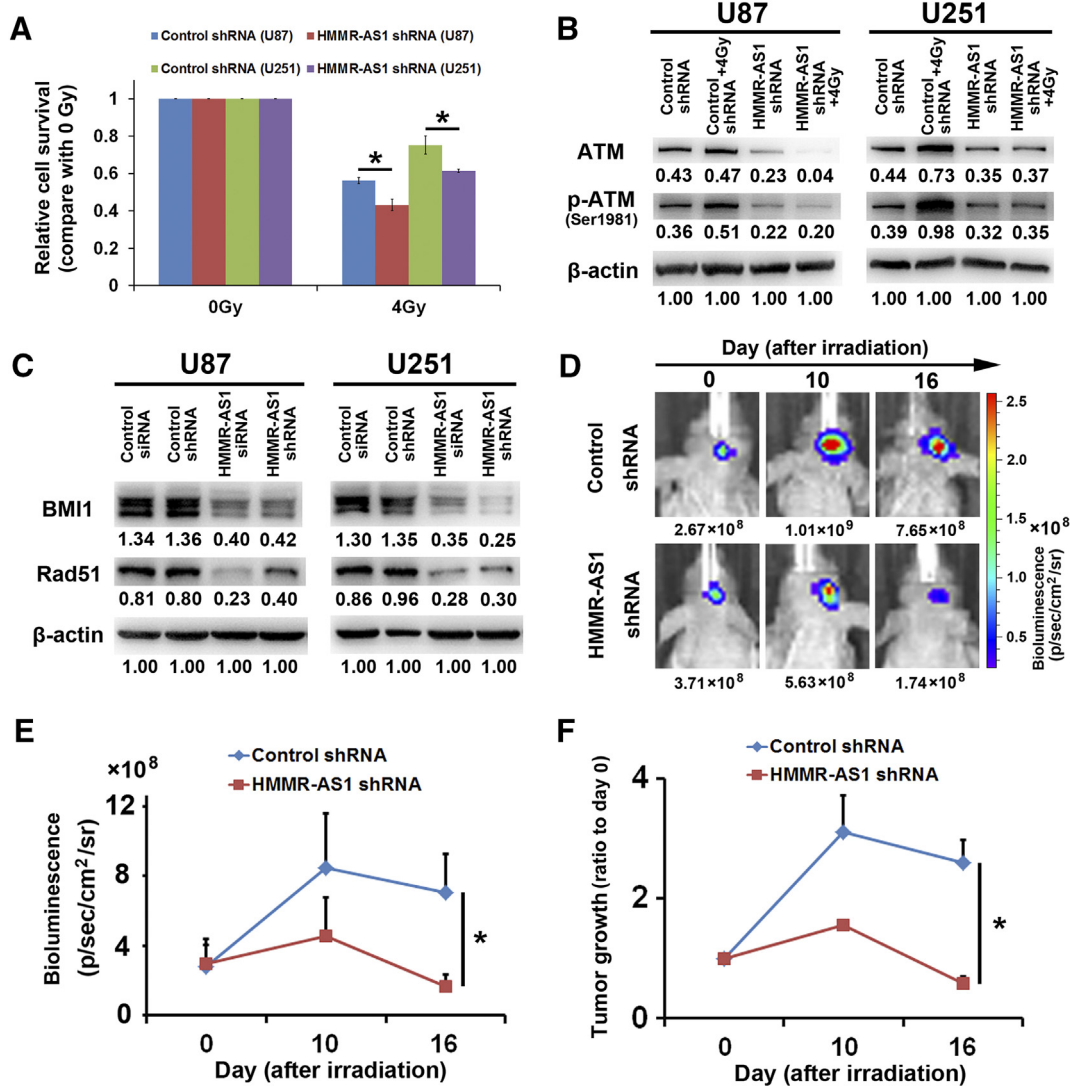


Figure 6. Knockdown of HMMR-AS1 sensitizes glioblastoma to X-ray irradiation *in vitro* and *in vivo*. U87 and U251 cells were transfected with control or HMMR-AS1 shRNA, and cells were exposed to 4-Gy X-ray irradiation. (A) Cell survival was detected using CCK-8 kit. (B) ATM and p-ATM levels were detected by using Western blot. (C) U87 and U251 cells were transfected with HMMR-AS1 siRNA or shRNA, and the expression of RAD51 and BMI1 was detected by using Western blot. (D) U87-luc cells transfected with a control shRNA or HMMR-AS1 shRNA were separately transplanted into the right striatum of nude mice. Mice were exposed to a total dosage of 12-Gy X-ray. (E) The bioluminescence signal was captured at day 10 and 16 postirradiation, and the signal intensity represented the size of transplanted tumor. (F) The growth curves of individual tumors were based on the ratios of bioluminescence signals to the baseline signals at day 0. β-Actin was used as a loading control. The blot bands were quantified by ImageJ and represented by relative values compare with loading control (1.00). **P* < .05.

HMMR-AS1 shRNA group (n = 3) than those in control group (n = 3) (Figure 5, A and B). The growth curves of individual tumors based on the ratios of bioluminescence signals to the baseline signals at day 6 indicated that the growth of tumors expressing HMMR-AS1 shRNA is significantly inhibited (Figure 5C). The IHC staining showed that expression of HMMR, β-Catenin, ZEB1, and Vimentin is decreased in tumor cells expressing HMMR-AS1 shRNA (Figure 5, D-F).

HMMR-AS1 Affects GBM Radiosensitivity

To investigate whether knockdown of HMMR-AS1 improves the cytotoxic effects of irradiation on GBM cells, U87 and U251 cells stably transfected with HMMR-AS1 shRNA were exposed to 4-Gy X-ray irradiation, and the cell growth was measured after 96 hours. We found that cells transfected with HMMR-AS1 shRNA were more sensitive to X-ray irradiation (Figure 6A).

Figure 5. Knockdown of HMMR-AS1 inhibits glioblastoma growth *in vivo*. U87-luc cells transfected with a control shRNA or HMMR-AS1 shRNA were separately transplanted into the right striatum of nude mice. Tumor growth was monitored by bioluminescence *in vivo* imaging. (A) The bioluminescence signal was captured at day 6, 12, 18, and 24 after cell implantation. (B) The signal intensity represented the size of transplanted tumor. (C) The growth curves of individual tumors were based on the ratios of bioluminescence signals to the baseline signals at day 6. (D) The H&E and IHC staining of HMMR for mice brain sections. Scale bar = 2 mm. (E) IHC staining showed that HMMR expression is decreased in tumors expressing HMMR-AS1 shRNA. Scale bar = 50 μm. (F) IHC staining showed that the expression of mesenchymal phenotypes β-Catenin, ZEB1, and Vimentin is decreased in tumors expressing HMMR-AS1 shRNA. Scale bar = 50 μm. **P* < .05.

To further reveal the mechanisms, we measured the expression of ATM, RAD51, and BMI1 in cells. ATM is the master kinase in the process of DNA repair responding to irradiation [22]. RAD51 and BMI1 are downstream of ATM and are required for efficient HR of DNA DSBs [23,24]. Our data showed that knockdown of HMMR-AS1 reduces expression of ATM and irradiation-increased phosphorylation of ATM (Figure 6B). Moreover, knockdown of HMMR-AS1 by either transiently transfected siRNA or stably transfected shRNA reduces the expression of RAD51 and BMI1 (Figure 6C).

Then, we assessed whether knockdown of HMMR-AS1 sensitizes GBM to X-ray irradiation *in vivo*. U87-Fluc reporter cells expressing HMMR-AS1 shRNA were orthotopically transplanted into the right striatum of nude mice. A total dosage of 12 Gy (3 Gy each day for 4 consecutive days) whole brain X-ray radiotherapy was administrated with a dedicated small animal radiotherapy device. The bioluminescence signal was captured at day 10 and 16 postirradiation (Figure 6D). The bioluminescence signals of individual tumors and the growth curves of tumors based on the ratios of signals to day 0 indicated that tumors expressing HMMR-AS1 shRNA ($n = 3$) are more sensitive to radiotherapy than control ($n = 3$) (Figure 6, E and F).

Discussion

As the partners of protein-coding genes, most antisense transcripts are noncoding in the mammalian genome, although some of them have been demonstrated to encode peptides [25–29]. Antisense transcripts are variously expressed in different tissues and cell lines and are not always linked to expression of the sense gene [13,30–32], indicating their complicated regulatory effects. Lots of functional antisense transcripts in mammalian genomes and the proposed mechanisms for antisense-mediated regulation of sense mRNA have been reported [33]. One noteworthy mechanism of antisense interfering sense is to alter sense mRNA stability and then regulate sense-encoded protein. A *BACE1* antisense transcript, *BACE1-AS*, has been found to be elevated in Alzheimer's disease and increases *BACE1* mRNA stability and protein expression [34]. Nature antisense transcript of inducible nitric oxide synthase gene has been reported to increase the stability of inducible nitric oxide synthase mRNA and participate in NO-mediating inflammatory diseases [35]. A *Sirt1* antisense lncRNA was found to interact with *Sirt1* mRNA, forming RNA duplex to stabilize *Sirt1* [36]. On the contrary, in cases of sense-antisense interaction, some antisense transcripts were identified to inhibit sense protein expression by stalling translation [37–39]. In the present study, we demonstrated that an *HMMR* antisense RNA, HMMR-AS1, is elevated in GBM cells and regulates *HMMR* expression. Knockdown of HMMR-AS1 reduced both *HMMR* mRNA and protein levels, whereas ectopic overexpression of HMMR-AS1 did not affect *HMMR* expression. Thus, we assumed that HMMR-AS1 may act to stabilize *HMMR* structurally rather than promote or stall its expression. To define the sense-antisense interference between *HMMR* and HMMR-AS1, we analyzed the stability of *HMMR* mRNA by using α -amanitin and found that knockdown of HMMR-AS1 destabilizes *HMMR* mRNA.

Since HMMR-AS1 is hyperexpressed in GBM cells, we investigated whether knockdown of HMMR-AS1 affects cell growth. We separately used siRNAs or shRNA targeting HMMR-AS1 to transfect GBM cells and found that knockdown of HMMR-AS1 suppresses cell growth both *in vitro* and *in vivo*. In U87 cells transfected with

HMMR-AS1 siRNA, cell cycle was blocked to pass the restriction (R) point which is necessary for G1 phase progression and S phase entry, and several cell cycle regulators (CDK2, CDK4, Cyclin D1, and p27 Kip1) were involved. We also found that knockdown of HMMR-AS1 reduces phosphorylation of ERK1/2 and expression of BMI1 and c-Myc. ERK1/2 and BMI1 have been reported as the downstream factors of HMMR in maintaining the malignancy of GBM [4]; thus, HMMR-AS1 may regulate ERK1/2 and BMI1 by altering HMMR expression. c-Myc functions as a transcriptional regulator with roles in cell proliferation and differentiation, and has been reported as a downstream regulator of ERK1/2 signaling in lung tumorigenesis [40]. Although no reported study ever mentioned whether HMMR can directly regulate c-Myc expression in GBM, we assumed that HMMR-AS1 may regulate c-Myc through HMMR/ERK1/2 signaling, yet further studies are needed to reveal the mechanisms. Moreover, we found that knockdown of HMMR-AS1 inhibits GBM cell migration, invasion, and the mesenchymal phenotypes. As a hyaluronan receptor, HMMR has ever been identified to be required for epicardial cell epithelial-mesenchymal transition (EMT) and migration [41]. Hyperexpression of HMMR has been reported to promote mitotic spindle formation and cell motility [42,43] and is associated with cancer aggressiveness, metastatic outgrowths, and poor prognosis [5,44]. Thus, HMMR-AS1 may affect cell migration and invasion by regulating HMMR expression.

Clinically, GBMs are characterized by resistance to radiotherapy. A major mechanism of radioresistance is through activation of DNA repair pathways responding to DNA DSBs [45,46]. ATM is the master regulator in DNA repair responses which plays critical roles in conferring GBM radioresistance, targeting which provides a strategy for GBM radiosensitization and growth control [47,48]. RAD51 and BMI1 are both ATM downstream DNA repair proteins involved in HR of DSBs [23,24,49]. RAD51 is overexpressed and contributes to radioresistance in malignant gliomas [50], and BMI1 is enriched in GBM cells as a component of the DNA damage response machinery [24,49]. Inhibition of RAD51 has been shown to radiosensitize glioma stem cells [51], and BMI1 deficiency in GBM cells severely impaired DNA DSB response, resulting in increased sensitivity to radiation [49]. Our study revealed that knockdown of HMMR-AS1 reduces irradiation-induced phosphorylation of ATM and the levels of RAD51 and BMI1, sensitizing GBM to X-ray irradiation *in vitro* and *in vivo*.

Conclusions

This study demonstrates that an *HMMR* antisense RNA, HMMR-AS1, is hyperexpressed in GBM cells and participates in cell growth, migration, and invasion by regulating HMMR expression. Knockdown of HMMR-AS1 suppresses and radiosensitizes GBM *in vitro* and *in vivo*. Our new findings reveal a mechanism of sense-antisense interference between *HMMR* and HMMR-AS1, provide a supportive evidence for targeting long noncoding RNA to GBM, and suggest HMMR-AS1 as a potential target for GBM treatment.

Financial Support

This work was supported by National Natural Science Foundation of China (grant numbers 81301905, 81672503); and Natural Science Foundation of Jiangsu Province (grant number BK20140731).

Acknowledgements

Not applicable.

Declarations of Interest

None.

References

- [1] Perry JR, Laperriere N, O'Callaghan CJ, Brandes AA, Menten J, Phillips C, Fay M, Nishikawa R, Cairncross JG, and Roa W, et al (2017). Short-course radiation plus temozolomide in elderly patients with glioblastoma. *N Engl J Med* **376**, 1027–1037. <https://doi.org/10.1056/NEJMoa1611977>.
- [2] Alexander BM and Cloughesy TF (2017). Adult Glioblastoma. *J Clin Oncol* **35**, 2402–2409. <https://doi.org/10.1200/JCO.2017.73.0119>.
- [3] Diamandis P and Aldape KD (2017). Insights From Molecular Profiling of Adult Glioma. *J Clin Oncol* **35**, 2386–2393. <https://doi.org/10.1200/JCO.2017.73.9516>.
- [4] Tilghman J, Wu H, Sang Y, Shi X, Guerrero-Cazares H, Quinones-Hinojosa A, Eberhart CG, Lattera J, and Ying M (2014). HMMR maintains the stemness and tumorigenicity of glioblastoma stem-like cells. *Cancer Res* **74**, 3168–3179. <https://doi.org/10.1158/0008-5472.CAN-13-2103>.
- [5] Rizzardi AE, Vogel RI, Koopmeiners JS, Forster CL, Marston LO, Rosener NK, Akentieva N, Price MA, Metzger GJ, and Warlick CA, et al (2014). Elevated hyaluronan and hyaluronan-mediated motility receptor are associated with biochemical failure in patients with intermediate-grade prostate tumors. *Cancer* **120**, 1800–1809. <https://doi.org/10.1002/cncr.28646>.
- [6] Wang C, Thor AD, Moore II DH, Zhao Y, Kerschmann R, Stern R, Watson PH, and Turley EA (1998). The overexpression of RHAMM, a hyaluronan-binding protein that regulates ras signaling, correlates with overexpression of mitogen-activated protein kinase and is a significant parameter in breast cancer progression. *Clin Cancer Res* **4**, 567–576.
- [7] Crainie M, Belch AR, Mant MJ, and Pilarski LM (1999). Overexpression of the receptor for hyaluronan-mediated motility (RHAMM) characterizes the malignant clone in multiple myeloma: identification of three distinct RHAMM variants. *Blood* **93**, 1684–1696.
- [8] Pujana MA, Han JD, Starita LM, Stevens KN, Tewari M, Ahn JS, Rennert G, Moreno V, Kirchhoff T, and Gold B, et al (2007). Network modeling links breast cancer susceptibility and centrosome dysfunction. *Nat Genet* **39**, 1338–1349. <https://doi.org/10.1038/ng.2007.2>.
- [9] Zheng Y, Liu L, and Shukla GC (2017). A comprehensive review of web-based non-coding RNA resources for cancer research. *Cancer Lett* **407**, 1–8. <https://doi.org/10.1016/j.canlet.2017.08.015>.
- [10] Bhan A, Soleimani M, and Mandal SS (2017). Long Noncoding RNA and Cancer: A New Paradigm. *Cancer Res* **77**, 3965–3981. <https://doi.org/10.1158/0008-5472.CAN-16-2634>.
- [11] Peng WX, Koirala P, and Mo YY (2017). LncRNA-mediated regulation of cell signaling in cancer. *Oncogene* **36**, 5661–5667. <https://doi.org/10.1038/ncr.2017.184>.
- [12] Evans JR, Feng FY, and Chinnaiyan AM (2016). The bright side of dark matter: lncRNAs in cancer. *J Clin Invest* **126**, 2775–2782. <https://doi.org/10.1172/JCI84421>.
- [13] Katayama S, Tomaru Y, Kasukawa T, Waki K, Nakanishi M, Nakamura M, Nishida H, Yap CC, Suzuki M, and Kawai J, et al (2005). Antisense transcription in the mammalian transcriptome. *Science* **309**, 1564–1566. <https://doi.org/10.1126/science.1112009>.
- [14] Boque-Sastre R, Soler M, Oliveira-Mateos C, Portela A, Moutinho C, Sayols S, Villanueva A, Esteller M, and Guil S (2015). Head-to-head antisense transcription and R-loop formation promotes transcriptional activation. *Proc Natl Acad Sci U S A* **112**, 5785–5790. <https://doi.org/10.1073/pnas.1421197112>.
- [15] Numata K and Kiyosawa H (2012). Genome-wide impact of endogenous antisense transcripts in eukaryotes. *Front Biosci (Landmark Ed)* **17**, 300–315.
- [16] Wang Q, Zhang J, Liu Y, Zhang W, Zhou J, Duan R, Pu P, Kang C, and Han L (2016). A novel cell cycle-associated lncRNA, HOXA11-AS, is transcribed from the 5-prime end of the HOXA transcript and is a biomarker of progression in glioma. *Cancer Lett* **373**, 251–259. <https://doi.org/10.1016/j.canlet.2016.01.039>.
- [17] Qin X, Yao J, Geng P, Fu X, Xue J, and Zhang Z (2014). LncRNA TSLC1-AS1 is a novel tumor suppressor in glioma. *Int J Clin Exp Pathol* **7**, 3065–3072.
- [18] Pastori C, Kapranov P, Penas C, Peschansky V, Volmar CH, Sarkaria JN, Bregy A, Komotar R, St Laurent G, and Ayad NG, et al (2015). The bromodomain protein BRD4 controls HOTAIR, a long noncoding RNA essential for glioblastoma proliferation. *Proc Natl Acad Sci U S A* **112**, 8326–8331. <https://doi.org/10.1073/pnas.1424220112>.
- [19] Zhang JX, Han L, Bao ZS, Wang YY, Chen LY, Yan W, Yu SZ, Pu PY, Liu N, and You YP, et al (2013). HOTAIR, a cell cycle-associated long noncoding RNA and a strong predictor of survival, is preferentially expressed in classical and mesenchymal glioma. *Neuro-Oncology* **15**, 1595–1603. <https://doi.org/10.1093/neuonc/not131>.
- [20] Mineo M, Ricklefs F, Rooj AK, Lyons SM, Ivanov P, Ansari KI, Nakano I, Chiocca EA, Godlewski J, and Bronisz A (2016). The long non-coding RNA HIF1A-AS2 facilitates the maintenance of mesenchymal glioblastoma stem-like cells in hypoxic niches. *Cell Rep* **15**, 2500–2509. <https://doi.org/10.1016/j.celrep.2016.05.018>.
- [21] Li J, Zhou Y, Wang H, Gao Y, Li L, Hwang SH, Ji X, and Hammock BD (2017). COX-2/SEH dual inhibitor PTUPB suppresses glioblastoma growth by targeting epidermal growth factor receptor and hyaluronan mediated motility receptor. *Oncotarget* **8**, 87353–87363. <https://doi.org/10.18632/oncotarget.20928>.
- [22] Blackford AN and Jackson SP (2017). ATM, ATR, and DNA-PK: The Trinity at the Heart of the DNA Damage Response. *Mol Cell* **66**, 801–817. <https://doi.org/10.1016/j.molcel.2017.05.015>.
- [23] Bakr A, Oing C, Kocher S, Borgmann K, Dornreiter I, Petersen C, Dikomey E, and Mansour WY (2015). Involvement of ATM in homologous recombination after end resection and RAD51 nucleofilament formation. *Nucleic Acids Res* **43**, 3154–3166. <https://doi.org/10.1093/nar/gkv160>.
- [24] Ginjała V, Nacerddine K, Kulkarni A, Oza J, Hill SJ, Yao M, Citterio E, van Luizuhen M, and Ganesan S (2011). BMI1 is recruited to DNA breaks and contributes to DNA damage-induced H2A ubiquitination and repair. *Mol Cell Biol* **31**, 1972–1982. <https://doi.org/10.1128/MCB.00981-10>.
- [25] Huang JZ, Chen M, Chen, Gao XC, Zhu S, Huang H, Hu M, Zhu H, and Yan GR (2017). A peptide encoded by a putative lncRNA HOXB-AS3 suppresses colon cancer growth. *Mol Cell* **68**, 171–184. <https://doi.org/10.1016/j.molcel.2017.09.015> [e6].
- [26] Anderson DM, Anderson KM, Chang CL, Makarewich CA, Nelson BR, McAnally JR, Kasaragod P, Shelton JM, Liou J, and Bassel-Duby R, et al (2015). A micropeptide encoded by a putative long noncoding RNA regulates muscle performance. *Cell* **160**, 595–606. <https://doi.org/10.1016/j.cell.2015.01.009>.
- [27] Nelson BR, Makarewich CA, Anderson DM, Winders BR, Troupes CD, Wu F, Reese AL, McAnally JR, Chen X, and Kavalali ET, et al (2016). A peptide encoded by a transcript annotated as long noncoding RNA enhances SERCA activity in muscle. *Science* **351**, 271–275. <https://doi.org/10.1126/science.aad4076>.
- [28] Matsumoto A, Pasut A, Matsumoto M, Yamashita R, Fung J, Monteleone E, Saghatelian A, Nakayama KI, Clohessy JG, and Pandolfi PP (2017). mTORC1 and muscle regeneration are regulated by the LINC00961-encoded SPAR polypeptide. *Nature* **541**, 228–232. <https://doi.org/10.1038/nature21034>.
- [29] Slavoff SA, Mitchell AJ, Schwaid AG, Cabili MN, Ma J, Levin JZ, Karger AD, Budnik BA, Rinn JL, and Saghatelian A (2013). Peptidomic discovery of short open reading frame-encoded peptides in human cells. *Nat Chem Biol* **9**, 59–64. <https://doi.org/10.1038/nchembio.1120>.
- [30] He Y, Vogelstein B, Velculescu VE, Papadopoulos N, and Kinzler KW (2008). The antisense transcriptomes of human cells. *Science* **322**, 1855–1857. <https://doi.org/10.1126/science.1163853>.
- [31] Okada Y, Tashiro C, Numata K, Watanabe K, Nakaoka H, Yamamoto N, Okubo K, Ikeda R, Saito R, and Kanai A, et al (2008). Comparative expression analysis uncovers novel features of endogenous antisense transcription. *Hum Mol Genet* **17**, 1631–1640. <https://doi.org/10.1093/hmg/ddn051>.
- [32] Wahlestedt C (2006). Natural antisense and noncoding RNA transcripts as potential drug targets. *Drug Discov Today* **11**, 503–508. <https://doi.org/10.1016/j.drudis.2006.04.013>.
- [33] Faghihi MA and Wahlestedt C (2009). Regulatory roles of natural antisense transcripts. *Nat Rev Mol Cell Biol* **10**, 637–643. <https://doi.org/10.1038/nrm2738>.
- [34] Faghihi MA, Modarresi F, Khalil AM, Wood DE, Sahagan BG, Morgan TE, Finch CE, St Laurent III G, Kenny PJ, and Wahlestedt C (2008). Expression of a noncoding RNA is elevated in Alzheimer's disease and drives rapid feed-forward regulation of beta-secretase. *Nat Med* **14**, 723–730. <https://doi.org/10.1038/nm1784>.
- [35] Matsui K, Nishizawa M, Ozaki T, Kimura T, Hashimoto I, Yamada M, Kaibori M, Kamiyama Y, Ito S, and Okumura T (2008). Natural antisense transcript

- stabilizes inducible nitric oxide synthase messenger RNA in rat hepatocytes. *Hepatology* **47**, 686–697. <https://doi.org/10.1002/hep.22036>.
- [36] Wang GQ, Wang Y, Xiong Y, Chen XC, Ma ML, Cai R, Gao Y, Sun YM, Yang GS, and Pang WJ (2016). Sirt1 AS lncRNA interacts with its mRNA to inhibit muscle formation by attenuating function of miR-34a. *Sci Rep* **6**, 21865. <https://doi.org/10.1038/srep21865>.
- [37] Hatzoglou A, Deshayes F, Madry C, Lapree G, Castanas E, and Tsapis A (2002). Natural antisense RNA inhibits the expression of BCMA, a tumour necrosis factor receptor homologue. *BMC Mol Biol* **3**, 4.
- [38] Mellin JR, Tiensuu T, Becavin C, Gouin E, Johansson J, and Cossart P (2013). A riboswitch-regulated antisense RNA in *Listeria monocytogenes*. *Proc Natl Acad Sci U S A* **110**, 13132–13137. <https://doi.org/10.1073/pnas.1304795110>.
- [39] Ebralidze AK, Guibal FC, Steidl U, Zhang P, Lee S, Bartholdy B, Jorda MA, Petkova V, Rosenbauer F, and Huang G, et al (2008). PU.1 expression is modulated by the balance of functional sense and antisense RNAs regulated by a shared cis-regulatory element. *Genes Dev* **22**, 2085–2092. <https://doi.org/10.1101/gad.1654808>.
- [40] Chou YT, Lin HH, Lien YC, Wang YH, Hong CF, Kao YR, Lin SC, Chang YC, Lin SY, and Chen SJ, et al (2010). EGFR promotes lung tumorigenesis by activating miR-7 through a Ras/ERK/Myc pathway that targets the Ets2 transcriptional repressor ERF. *Cancer Res* **70**, 8822–8831. <https://doi.org/10.1158/0008-5472.CAN-10-0638>.
- [41] Missinato MA, Tobita K, Romano N, Carroll JA, and Tsang M (2015). Extracellular component hyaluronic acid and its receptor Hmhr are required for epicardial EMT during heart regeneration. *Cardiovasc Res* **107**, 487–498. <https://doi.org/10.1093/cvr/cvv190>.
- [42] Maxwell CA, Keats JJ, Crainie M, Sun X, Yen T, Shibuya E, Hendzel M, Chan G, and Pilarski LM (2003). RHAMM is a centrosomal protein that interacts with dynein and maintains spindle pole stability. *Mol Biol Cell* **14**, 2262–2276. <https://doi.org/10.1091/mbc.E02-07-0377>.
- [43] Dunsch AK, Hammond D, Lloyd J, Schermelleh L, Gruneberg U, and Barr FA (2012). Dynein light chain 1 and a spindle-associated adaptor promote dynein asymmetry and spindle orientation. *J Cell Biol* **198**, 1039–1054. <https://doi.org/10.1083/jcb.201202112>.
- [44] Stevens LE, Cheung WKC, Adua SJ, Arnal-Estape A, Zhao M, Liu Z, Brewer K, Herbst RS, and Nguyen DX (2017). Extracellular matrix receptor expression in subtypes of lung adenocarcinoma potentiates outgrowth of micrometastases. *Cancer Res* **77**, 1905–1917. <https://doi.org/10.1158/0008-5472.CAN-16-1978>.
- [45] Marampon F, Megiorni F, Camero S, Crescioli C, McDowell HP, Sferra R, Vetuschi A, Pompili S, Ventura L, and De Felice F, et al (2017). HDAC4 and HDAC6 sustain DNA double strand break repair and stem-like phenotype by promoting radioresistance in glioblastoma cells. *Cancer Lett* **397**, 1–11. <https://doi.org/10.1016/j.canlet.2017.03.028>.
- [46] Mukherjee B, McEllin B, Camacho CV, Tomimatsu N, Sirasanagandala S, Nannepaga S, Hatanpaa KJ, Mickey B, Madden C, and Maher E, et al (2009). EGFRvIII and DNA double-strand break repair: a molecular mechanism for radioresistance in glioblastoma. *Cancer Res* **69**, 4252–4259. <https://doi.org/10.1158/0008-5472.CAN-08-4853>.
- [47] Ahmed SU, Carruthers R, Gilmour L, Yildirim S, Watts C, and Chalmers AJ (2015). Selective Inhibition of Parallel DNA Damage Response Pathways Optimizes Radiosensitization of Glioblastoma Stem-like Cells. *Cancer Res* **75**, 4416–4428. <https://doi.org/10.1158/0008-5472.CAN-14-3790>.
- [48] Vecchio D, Daga A, Carra E, Marubbi D, Raso A, Mascelli S, Nozza P, Garre ML, Pitto F, and Ravetti JL, et al (2015). Pharmacokinetics, pharmacodynamics and efficacy on pediatric tumors of the glioma radiosensitizer KU60019. *Int J Cancer* **136**, 1445–1457. <https://doi.org/10.1002/ijc.29121>.
- [49] Facchino S, Abdouh M, Chatoo W, and Bernier G (2010). BMI1 confers radioresistance to normal and cancerous neural stem cells through recruitment of the DNA damage response machinery. *J Neurosci* **30**, 10096–10111. <https://doi.org/10.1523/JNEUROSCI.1634-10.2010>.
- [50] Short SC, Giampieri S, Worku M, Alcaide-German M, Sioftanos G, Bourne S, Lio KI, Shaked-Rabi M, and Martindale C (2011). Rad51 inhibition is an effective means of targeting DNA repair in glioma models and CD133+ tumor-derived cells. *Neuro-Oncology* **13**, 487–499. <https://doi.org/10.1093/neuonc/nor010>.
- [51] King HO, Brend T, Payne HL, Wright A, Ward TA, Patel K, Egnuni T, Stead LF, Patel A, and Wurdak H, et al (2017). RAD51 is a selective DNA repair target to radiosensitize glioma stem cells. *Stem Cell Rep* **8**, 125–139. <https://doi.org/10.1016/j.stemcr.2016.12.005>.